Energy relaxation rates in dense hydrogen plasmas

B. Jeon,[1,2] M. Foster,[1] J. Colgan,[1] G. Csanak,[1] J. D. Kress,[1] L. A. Collins,[1] and N. Grønbech-Jensen[2]
[1]*Theoretical Division, Los Alamos National Laboratory, Los Alamos, New Mexico 87545, USA*
[2]*Department of Applied Science, University of California, Davis, California 95616, USA*
(Received 9 May 2008; published 12 September 2008)

A comprehensive study is made of the energy relaxation rates between ions and electrons in a dense hydrogen plasma. Results of classical molecular dynamics (MD) simulations are compared with quantal calculations using the Fermi golden rule and using dimensional continuation. The rates from the molecular dynamics simulations employing a screened potential are found to be in reasonable agreement with the Landau-Spitzer relaxation rates, and are around 30% higher than the Fermi golden rule rates. By inverting the classical MD relaxation rate vs the quantal result, a semiclassical value for the screening length is suggested. We present energy relaxation rates relevant for radiation-hydrodynamic simulations of inertial confinement fusion devices.

DOI: 10.1103/PhysRevE.78.036403 PACS number(s): 52.27.−h

I. INTRODUCTION

The rate at which energy is transferred between electrons and ions is a quantity of fundamental importance in nonequilibrium plasmas. In particular, radiation-hydrodynamic simulations of dense plasmas, such as those found in inertial-confinement-fusion (ICF) devices, require accurate energy transfer rates in order to model properly the energy and momentum transfer in the system. The theoretical study of such energy relaxation rates has a long history, beginning with the pioneering work of Landau and Spitzer [1–3], who considered weakly coupled plasmas under classical conditions. Generalizations of this approach for lower temperature plasmas were made by Brysk [4], and further improved by Lee and More [5]. More recently, Dharma-wardana and Perrot [6,7] derived a relaxation rate by drawing an analogy with the work of Kogan [8], who applied the Fermi golden rule to metals and semiconductors. Consideration of the coupled-mode behavior of the plasma has permitted further extensions [7]. An intuitive derivation of the Kogan approach as applied to weakly coupled electron-ion systems was also given by Hazak *et al.* [9], who introduced a modification of the Kogan expression that reduces to the Landau-Spitzer result in the high temperature region. Various quantum-kinetic approaches have been proposed to describe the energy relaxation for strongly coupled systems [10,11], which may avoid the requirement of cutoff parameters in the Coulomb logarithm. Recently, the application of dimensional continuation has yielded an analytic expression for the electron-ion relaxation rate [12,13] of a fully ionized weakly coupled plasma. Further, an analytic expression of the energy relaxation rate for nonequilibrium systems has recently been presented [14].

Experimental determinations of electron-ion relaxation rates are notoriously difficult. Two main approaches have been taken: (i) the use of short, intense laser pulses to produce hot electrons and cool ions, or (ii) the use of shock compression devices to heat the ions with corresponding cool electrons. Early experiments by the Ng group [15,16], using the latter approach with a Si plasma suggested that the electron temperature was much less than the ion temperature, but the extraction of a relaxation rate proved inconclusive. Riley *et al.* [17] measured absolute x-ray scattering cross sections from dense Al plasmas created by strong laser-driven shocks. The measured cross sections were in disagreement with hydrodynamic simulations suggesting that the Landau-Spitzer energy relaxation rate used in the simulations may be inaccurate. These indirect experiments further underscored the importance of understanding the energy relaxation rates between electrons and ions in dense plasmas. Efforts are underway at Los Alamos National Laboratory to measure the temperatures of both electrons and ions in a strongly coupled plasma to obtain a direct measurement of the relaxation rate [18], as well as at the OMEGA laser facility at the University of Rochester and the National Ignition Facility at Lawrence Livermore National Laboratory to measure electron-ion coupling rates in hot, dense plasmas.

We present large-scale molecular dynamics (MD) simulations of the electron-ion relaxation rate for conditions typical of ICF. Due to a lack of experimental data for these conditions, our only recourse is to perform MD simulations where Newton's equations of motion are integrated for ions and electrons interacting through a well-defined potential to describe the interparticle forces. In addition, we have examined the sensitivity of the relaxation process to various parameters in the potential. Such a study provides a critical assessment of certain "quantal" enhancements of the bare Coulomb interaction. Previous MD simulations have been used to study energy relaxation in strongly coupled systems [19–21], but typically only included a very limited number (10^2) of particles. We demonstrate the ability of classical MD simulations to include on the order of 10^6 particles using contemporary high-performance computing. We complement these "numerical experiments" with calculations using the quantum-mechanical Fermi golden rule method of Dharma-wardana and Perrot [6,7] and Hazak *et al.* [9], which is appropriate because we only consider weakly coupled systems. In the following, we first describe our numerical methods and results, before giving a detailed discussion of the comparison of the relaxation rate from MD simulations and from quantal approaches.

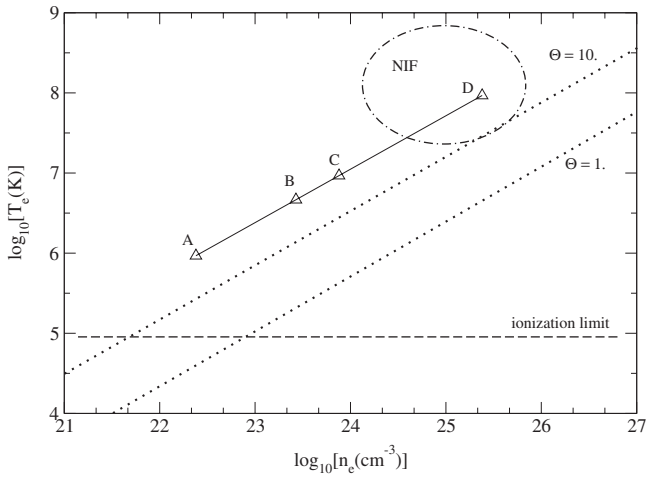

FIG. 1. Phase diagram of a hydrogen plasma. Various values of the degeneracy parameter Θ of the plasma are indicated. The fuel core of NIF exists in the region within the ellipse. The MD simulations were performed for points A–D as discussed in the text.

II. THEORETICAL METHODS

A. Molecular dynamics simulations

For hydrogen, the ionization energy is 13.595 eV [22], and the ionization limit is 1.0518×10^5 K. The plasma degeneracy $\Theta=\frac{k_BT}{E_F}$, where E_F is the Fermi energy, is a guide to whether the system exists in a classical or quantum state. If $\Theta>10$, electrons exist in the fully nondegenerate region and can be described by classical methods except for short-range collisions [23]. These regions are illustrated on the phase diagram shown in Fig. 1, which indicates selected test points for which MD simulations were performed. These points lie along the same degeneracy line. For completeness, we also list, in Table I, the various plasma parameters for each point indicated in Fig. 1, along with various constants of the plasma. All the points considered lie well above the ionization limit and are well within the region for which classical MD simulations are appropriate.

For our MD simulations, we adopt a bare Coulomb potential for the repulsive electron-electron and ion-ion interactions while a Deutsch potential [24] is used for the attractive electron-ion interactions as

$$V_{ei}=\frac{q_eq_ie^2}{4\pi\epsilon_0}\frac{1}{r}\left[1-\exp\left(-\frac{r}{r_s}\right)\right], \tag{1}$$

where the characteristic distance r_s is the thermal de Broglie wavelength [$\lambda_{ei}=h/\sqrt{2\pi mkT}$, where T is the average temperature $T=0.5(T_e+T_i)$, and m is the electron mass]. To simulate the given system efficiently, a parallel MD code has been developed employing periodic boundary conditions. A conventional velocity Verlet integrator propagates the equations of motion within the microcanonical and isokinetic ensembles. A particle mesh Ewald algorithm incorporates periodic images of Coulomb interactions; particle interactions are calculated for all pairs for small ensembles or by a cell-sorting method for large ones. Pipe-lining or domain decomposition is employed for the parallel direct sum and a parallel fast-fourier transform (FFT) is used for the reciprocal sum. The details of the implemented MD simulations can be found in [25].

To achieve full relaxation requires more than 10^9 time steps. Simulations for only partial relaxation still require a very large number of time steps ($\geqslant10^7$). This computational difficulty has necessitated the adoption of two approaches. First, we employ samples of several thousand particles to examine the early relaxation behavior of the electron-proton plasma. For statistical reliability, it would be preferable to employ samples of around a million particles, but the vast number of time steps required makes this choice impractical. Second, we employ an acceleration procedure, which entails using a reduced ion mass of 0.01 amu instead of the real proton mass of 1.0 amu. This reduced mass ratio accelerates

TABLE I. *e-H* plasma system configurations. The subscript *e* indicates an electron parameter while *i* indicates an ion parameter. Other quantities listed include n for number density, T for initial temperature, λ_{Debye} for Debye screening length ($\lambda_{\text{Debye}}=\sqrt{kT/4\pi ne^2}$), a for Wigner-Seitz radius, Γ for the plasma coupling constant, λ_{ei} for the thermal de Broglie wavelength [$\lambda_{ei}=h/\sqrt{2\pi mkT}$, $T=0.5(T_e+T_i)$], and ω for the plasma frequency.

Symbol	A	B	C	D	Unit
n_e	2.4×10^{22}	2.680×10^{23}	7.590×10^{23}	2.4×10^{25}	cm^{-3}
n_i	2.4×10^{22}	2.680×10^{23}	7.590×10^{23}	2.4×10^{25}	cm^{-3}
T_e	80	400	800	8,000	eV
T_i	100	500	1,000	10,000	eV
$\lambda_{\text{Debye\_e}}$	4.292	2.872	2.414	1.357	Å
$\lambda_{\text{Debye\_i}}$	4.799	3.211	2.698	1.518	Å
a_e, a_i	2.151	9.622×10^{-1}	6.801×10^{-1}	2.151×10^{-1}	Å
Γ_e	8.369×10^{-2}	3.741×10^{-2}	2.647×10^{-2}	8.369×10^{-3}	
Γ_i	6.696×10^{-2}	2.993×10^{-2}	2.117×10^{-2}	6.696×10^{-3}	
λ_{ei}	7.296×10^{-1}	3.263×10^{-1}	2.307×10^{-1}	7.296×10^{-2}	Å
ω_e	8.740×10^{15}	2.921×10^{16}	4.915×10^{16}	2.764×10^{17}	Hz

the relaxation by more than a factor of 10 and so allows us to accommodate much larger systems ($\sim 10^6$ particles) with high statistical accuracy.

By analyzing the MD simulations, the physical properties of the electron-proton plasma can be investigated. To find the relaxation rate from the results of molecular dynamics, the fitting scheme of [19,20] is used. Assuming exponential decay of the electron temperature difference, we can fit the transient change with a time constant τ_H as

$$dT_e/dt \sim \exp(-t/\tau_h), \tag{2}$$

which relates to the relaxation rate g through

$$g = \frac{3}{2}\frac{dT_e/dt}{\Delta T}k_B = \frac{3}{4}\frac{k_B}{\tau_H}. \tag{3}$$

That is, g will be proportional to the inverse of the time constant τ_H.

B. Landau-Spitzer

The Landau-Spitzer (LS) result [1–3] has the form

$$\frac{dE_e}{dt} = g(T_i - T_e), \tag{4}$$

where E_e is the total electron energy, and where the relaxation rate g is

$$g = \frac{3}{2}n_i\sqrt{2\pi}e^4\frac{8Z^2n_e}{3m_em_iT^{3/2}}\ln\Lambda_{LS}, \tag{5}$$

and where

$$T = \frac{T_e}{m_e} + \frac{T_i}{m_i}. \tag{6}$$

The relaxation rate contains the Coulomb logarithm, defined as $\ln\Lambda_{LS}=\int_{b_{\min}}^{b_{\max}}dk/k$. In the above expression, n_i is the number of ions (with charge Z) in the system with mass m_i, n_e is the electron density with mass m_e, and T_e (T_i) is the electron (ion) temperature. In this work we have used as $b_{\max}$ the electron Debye screening length ($\lambda_{\text{Debye}}=\sqrt{kT/4\pi ne^2}$), and as $b_{\min}$ the deBroglie wavelength [i.e., $\lambda_{ei}=h/\sqrt{2\pi mkT}$, $T=0.5(T_e+T_i)$]. We choose this value of $b_{\min}$ in order to best compare with our MD simulations, which were made with a screened potential with $r_s=\lambda_{ei}$. Other choices for b_{min} include $b_{min}=\lambda_{ei}/2\pi$ [20] and $b_{min}\sim 0.18\lambda_{ei}$ as derived from the analytical expression from dimensional continuation [12,13]. Lee and More [5] have improved the LS expression by incorporating additional degeneracy effects.

C. Fermi golden rule approach

The Fermi golden rule gives the following expression for the energy relaxation rate of a two-temperature plasma [6,7]:

$$\frac{dE_e}{dt} = \int_0^\infty \frac{d\omega}{2\pi}\omega\int\frac{d^3q}{(2\pi)^3}|U_{ie}(\mathbf{q})|^2\Delta N_{ie}A^eA^i, \tag{7}$$

where

$$\Delta N_{ie} = N_i(\omega/T_i) - N_e(\omega/T_e),$$

$$A^e = -2\,\mathrm{Im}[\chi_{ee}(q,\omega,T_e)],$$

$$A^i = -2\,\mathrm{Im}[\chi_{ii}(q,\omega,T_i)], \tag{8}$$

with $\chi_{ee}(q,\omega,T_e)$ and $\chi_{ii}(q,\omega,T_i)$ referring to the dynamical linear response function of the electron and ion subsystems, respectively. The Bose factors are given by $N_a(\omega/T_a)=[\exp(\omega/T_a)-1]^{-1}$ ($a=i$ or e). In expressions (7) and (8), q is the momentum transfer between the electrons and ions, and $\hbar\omega$ is the energy transferred. $U_{ie}(\mathbf{q})$ is the electron-ion interaction potential. In each equation atomic units have been used, and therefore Eq. (7) refers to the energy relaxation rate in one atomic unit of volume.

In general the ions are screened composite particles, and therefore $U_{ie}(\mathbf{q})$ is an effective interaction or "pseudopotential" [6,7]. The electron-ion interaction potential used in Eq. (7) can be derived from an average-atom treatment [26]. However, for the case of a fully ionized plasma, a much simpler Coulomb potential for the electron-ion interaction potential pertains yielding considerable speedup in the computation of the relaxation rates for a wide range of densities and temperatures. We also employ an average-atom method [26] to verify that the plasma is indeed fully ionized for a given temperature and density. Once this has been confirmed, a Coulomb potential may be used for $U_{ie}(\mathbf{q})$ in Eq. (7). The option of using a screened potential from average-atom codes for partially ionized plasmas is also in place. The electron linear response functions χ_{ee} are obtained fully quantum mechanically by using the random-phase approximation with local field corrections [23,27,28], whereas the ion linear response functions χ_{ii} are obtained from a semiclassical approach [29]. Thus the electron-electron and ion-ion couplings are treated to all orders while the electron-ion coupling is treated to first order, which for the weakly coupled systems (see Table I) under consideration here is appropriate.

As discussed by Hazak *et al.* [9], this approach may be further simplified in the cases where the spectrum of fluctuations of the ions is small compared with the electron and ion temperatures. In such a limit, the f-sum rule may be used to compute the integral over ω in Eq. (7) analytically. By linearizing the Bose factors so that $N_a \approx T_a/\omega$ the relaxation rate g can be written as

$$g = 4\int\frac{d^3q}{(2\pi)^3}|U_{ei}(\mathbf{q})|^2\left.\frac{\mathrm{Im}[\chi_{ee}(q,\omega,T_e)]}{\omega}\right|_{\omega=0}\frac{n_iq^2}{4m_i}. \tag{9}$$

This expression is numerically more convenient to evaluate than the original Fermi golden rule formula since it contains only a single integral over smooth functions instead of a double integral over sharply peaked functions [30].

III. RESULTS

A. Results of MD simulations

We performed MD simulations with 1536 electrons and 1536 protons for more than 10^7 time steps using the full bare

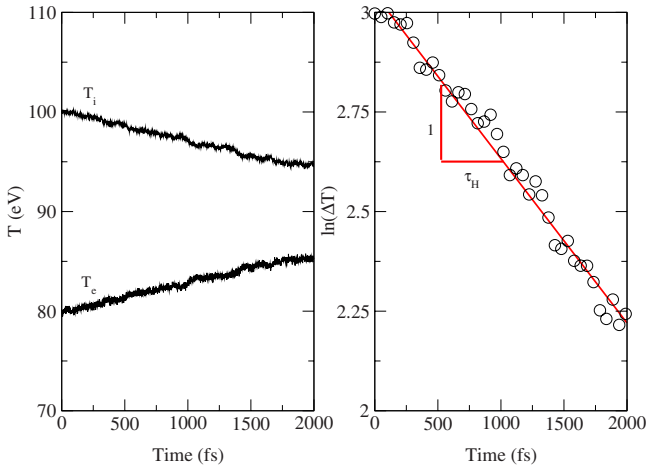

FIG. 2. (Color online) Bare proton mass simulations. Temperature curves (left) and logarithmic curves (right) of the temperature difference between the ions and electrons for test point A.

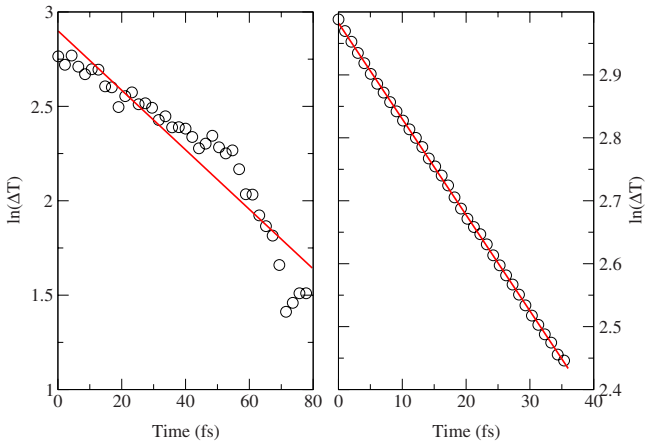

FIG. 3. (Color online) Temperature differences $\Delta T(=T_i-T_e)$ from the reduced ion mass simulations, for sampling point A. The left panel shows the temperature difference using 1536/1536 particles, and the right panel shows the temperature difference when $5\times10^5/5\times10^5$ particles are used.

ion mass. We first thermalize the system by isothermal simulations, using an isokinetic or stochastic thermostat, to evolve the sample for more than 10^5 time steps from given initial conditions. After this pretreatment, the electrons and protons are relaxed without any thermostat toward a microcanonical ensemble. By momentum transfer, the electron temperature increases while the ion temperature decreases. The temperatures converge toward an intermediate (approximately average) temperature but, as previously discussed, this process takes an impractical amount of computational resources to reach the equilibrium state. Therefore we only consider partial relaxation and use linear fitting to find a time constant for the evolution of the temperature differences.

Temporal relaxation is shown in Fig. 2 for point A, which shows an approximately linear temperature decay. From the fitting curve, we calculate the time constant as an inverse of the gradient. Points B and C are tested in the same way. However, we failed to extract any physical values from point D, which has extreme conditions of temperature and density. The acquired statistics for D were not sufficient, even with 10^8 time steps. Consequently, point D was studied quantitatively using the reduced mass simulations only.

To improve the statistics, simulations including 1 000 000 particles are required. By faster momentum exchange, the method of reduced ion mass decreases the required number of time steps by one to two orders of magnitude. In a subsequent series of simulations, we tested two different ensembles of particles. As done in the full ion mass cases, 1536 pairs of electrons and ions are simulated with all pairwise interactions [25]. In addition to these simulations, 5×10^5 pairs of electrons and ions were tested. This large particle set provides much better statistics and serves as a reference.

Results for sampling point A described in Table I are shown in Fig. 3. The curve on the left is the result from 1536 pairs whereas the curve on the right is for 5×10^5 pairs. Even though the 1536 pair simulations display considerable noise, as in the bare ion mass simulations, the fitted results show good agreement with the 5×10^5 pair simulations. For the 5×10^5 pairs of electrons and ions, we find nearly linear curves, implying sufficiently good statistics. Table II shows the time constant and rms error of the time constant fit for each MD simulation. We note that this is not the error in the MD simulation itself. For the larger system, the rms error clearly decreases. However, the time constant for point D is much larger when simulating 5×10^5 pair particles, than for the simulations using 1536 pairs. Even with the reduced ion mass simulations, the required time steps were too many for 5×10^5 particle pairs, and we could test only less than 1 fs, which may yield insufficient thermal mixing. Therefore we used the results of 1536 particle pairs of point D when comparing to other calculations.

B. Comparison of MD simulations with other methods

The comparison of our MD simulations with other calculations are presented in Tables III and IV. Although it is

TABLE II. Rms error and time constant of each MD simulation using the reduced-mass ion simulations. The number of electrons and ions employed is given within the parentheses. The unit of τ_H is fs.

Method	A	B	C	D
Rms error (1536)	1.354×10^{-1}	1.768×10^{-1}	5.973×10^{-2}	2.473×10^{-2}
Rms error (5×10^5)	2.499×10^{-3}	4.027×10^{-3}	1.681×10^{-3}	3.356×10^{-4}
τ_H (1536)	63.432	46.960	39.909	17.886
τ_H (5×10^5)	65.583	48.154	41.882	78.950

possible to recast the results from our MD simulations in terms of $\ln\Lambda$, we choose instead to compare the actual relaxation rate g, so that we can compare to quantal approaches as described previously.

In Table III we compare the MD simulations made using the bare ion mass, and 1536/1536 electrons and ions, with calculations using the modified Fermi golden rule method as defined in Eq. (9), with both an electron-ion potential derived from an average-atom treatment (MFGRAA) [26] and a Coulomb potential (MFGRC). This latter calculation assumes that the plasma is completely ionized. We also compare our calculations with the analytic expression of Brown *et al.* [12] (labeled BPS) and with the Landau-Spitzer formula of Eq. (5). The MD simulations produce relaxation rates in good agreement with the other approaches. For example, the MD rates are within 21% or better of the Landau-Spitzer rates. The amount of disagreement is not due to the error (better than 0.4% for 5×10^6 ions as shown in Table II) in the fitting of the relaxation time constant. This agreement is comparable to that obtained between MD simulations and the Landau-Spitzer formula for plasmas with stronger coupling [20] (Γ_i=0.4–2.3 and Γ_e=0.2–0.9), where the MD simulations employed the Deutsch potential, Eq. (1). The MFGRC results, assuming a fully ionized plasma, are in very good agreement with the results from the method of Brown *et al.* [12], who also made the assumption of a fully ionized plasma. The MFGRAA rates are slower than the MFGR calculations using a Coulomb potential, even though the average-atom treatment found that the plasma is between 93% and 98% ionized, depending on the test point. This highlights the extreme sensitivity of the relaxation rate to the choice of electron-ion potential. We also compare the Fermi golden rule calculations with the results from the Landau-Spitzer approach, and find that the latter predicts about a 40% lower relaxation rate compared to MFGRC and BPS.

Conceivably the MD results in Table III show a smaller relaxation rate than the MFGR and BPS calculations because of the relatively low number of particles used. We test this condition by comparing in Table IV similar simulations made with the reduced ion mass. In this case we can contrast the MD simulations of 1536 pairs of electrons and ions with the results of 5×10^5 pairs. For test points A, B, and C, the MD relaxation rate is insensitive to the number of particles, whereas for point D, the $5\times10^5/5\times10^5$ simulation appears questionable, as previously discussed.

For test points A, B, and C, the MD rates are significantly slower than the Landau-Spitzer (LS) rates. For the ratios of m_i/m_e considered in the present work (m_i/m_e=1837 for the bare mass calculations and m_i/m_e=18.37 for the reduced mass calculations), the Landau-Spitzer formula, Eq. (5), for the ratio of the relaxation rate $g(m_2)/g(m_1)$ to first order scales linearly as the inverse mass ratio m_1/m_2 of the ion masses m_1 and m_2. The deviation from first order for $g(\text{reduced,LS})/g(\text{bare,LS})$ is about 10%, as deduced from the results in Tables III and IV. Previous MD simulations of temperature relaxation in two-component plasmas with $\Gamma_i\sim2$, found [21] that $g(m_2)/g(m_1)$ scaled as $(m_1/m_2)^{0.86}$, and not $(m_1/m_2)^1$, for a range of mass ratios from 10 to 1000. If we assume this scaling for the present MD simulations then $g(\text{reduced,MD})/g(\text{bare,MD})=100^{0.86}=52$. Assuming in the limit of large m_i/m_e that $g(\text{bare,MD})=g(\text{bare,LS})$ and using $g(\text{reduced,LS})/g(\text{bare,LS})=90$ (Tables III and IV), this yields a predicted MD rate, $g(\text{reduced,MD})$ of 1.73 (=90/52) times slower than $g(\text{reduced,LS})$. This predicted slower MD rate is comparable to the actual slower MD rates in Tables III and IV (which are about 1.8–2.5 times slower relative to LS).

We note that, as in Table III, the MFGRC calculations are in very good agreement with the BPS calculations of [12] and that the Landau-Spitzer approach provides around a 40% lower relaxation rate compared to the MFGRC and BPS rates. In comparing Tables III and IV, we find that the MFGRC, BPS, and Landau-Spitzer rates scale to first order with the inverse of the ion mass (i.e., the rates in Table IV are about 100 times larger than the rates in Table III), as expected from inspection of Eqs. (5) and (9).

It should also be emphasized that previous studies [10] have shown the extreme sensitivity of the relaxation rate to the choice of $b_{\min}$ in the expression for $\ln\Lambda$ in Eq. (5). For example, if one uses a $b_{\min}$ value of $\lambda_{ei}/2\pi$, the Landau-

TABLE III. Relaxation rate g (W/K m^3) for test points defined in Fig. 1 using the bare ion mass simulations. The MD simulations employed 1536 electrons and 1536 ions. MFGRAA refers to the modified Fermi golden rule calculations made using Eq. (9), and using an electron-ion potential derived from an average-atom treatment [26]. MFGRC refers to the same calculations but using a Coulomb potential. BPS refers to the calculations of [12]. The numbers in the first row indicate the factor by which each column should be multiplied.

	A$\times10^{17}$	B$\times10^{18}$	C$\times10^{18}$	D$\times10^{20}$
MD	1.03	0.98	4.06	
MFGRAA	0.88	1.40	4.62	1.74
MFGRC	1.57	1.91	5.81	2.13
BPS [12]	1.53	1.94	5.79	2.14
Landau-Spitzer	0.90	1.24	3.81	1.51

TABLE IV. Relaxation rate g (W/K m^3) for test points defined in Fig. 1 using reduced ion mass simulations. The MD simulations employed the number of electrons and ions given within the parentheses. MFGRAA refers to the modified Fermi golden rule calculations made using Eq. (9), and using an electron-ion potential derived from an average-atom treatment [26]. MFGRC refers to the same calculations but using a Coulomb potential. BPS refers to the calculations of [12]. The numbers in the first row indicate the factor by which each column should be multiplied.

	A$\times10^{19}$	B$\times10^{20}$	C$\times10^{20}$	D$\times10^{22}$
MD (1536)	0.39	0.54	1.97	1.39
MD (5×10^5)	0.38	0.58	1.88	0.32
MFGRAA	0.84	1.42	4.71	1.92
MFGRC	1.57	1.91	5.81	2.13
BPS [12]	1.53	1.94	5.79	2.14
Landau-Spitzer	0.82	1.13	3.45	1.37

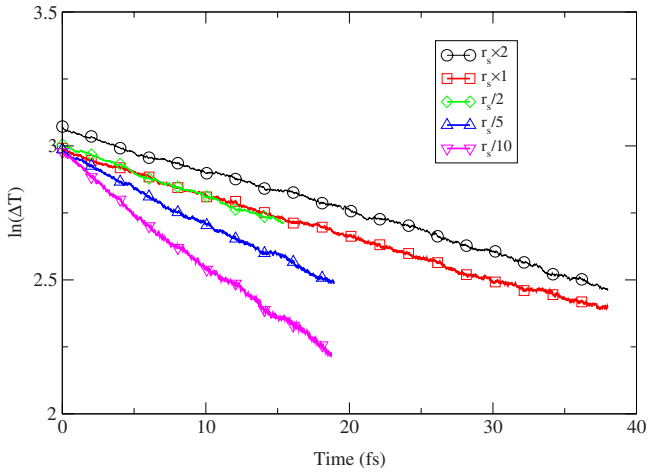

FIG. 4. (Color online) Temporal relaxation times for the conditions in test point A, using reduced ion masses and with 50 000/50 000 particles. Each simulation uses a different r_s value as described in the text.

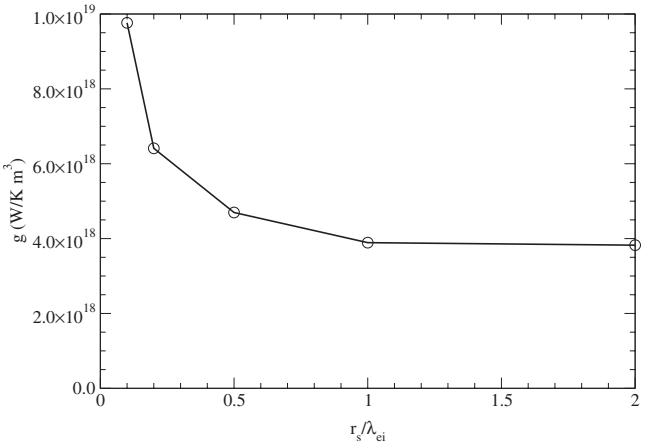

FIG. 5. Relaxation rate g as a function of r_s, for MD simulations made for the conditions in test point A using a reduced ion mass. See text for details.

Spitzer relaxation rate can increase by almost a factor of 2. A further discussion of this sensitivity can be found in Ref. [10]. This sensitivity does not arise in the MFGRC approaches, where the de Broglie wavelength or $\ln \Lambda$ does not appear explicitly. Although it has been shown that [9,14], in the high temperature limit, the MFGRC approach can be reduced to an expression analogous to the Landau-Spitzer expression Eq. (5) (i.e., with a $\ln \Lambda$ term), this reworking does not offer any guidance as to what $b_{\min}$ should be in this case.

C. The effect of the Deutsch parameter

In order to shed some light on the differences between the classical MD simulations and the results of the quantal approaches (MFGRC and [12]), we studied the effect of the Coulomb screening in the MD simulations, which is through the Deutsch potential [Eq. (1)]. The parameter r_s, which is set equal to the thermal de Broglie wavelength (λ_{ei}) in all MD simulations presented so far, determines the rate of the electron-ion collisions. To study the effect of r_s on the relaxation rate, several tests have been done in which we ran one final series of MD simulations for test point A. The reduced ion mass, 50 000 ions and 50 000 electrons, and several r_s values (0.1, 0.2, 0.5, 1.0, and $2.0 \times \lambda_{ei}$) were employed. The temporal relaxation curves are presented in Fig. 4. A smaller r_s expedites the momentum transfer between electrons and ions and the thermal mixing is faster. The relaxation rate (g) has been calculated for each value of r_s, and the results shown in Fig. 5. For $r_s = 2\lambda_{ei}$, the difference in the relaxation rate is negligible compared with $r_s = \lambda_{ei}$. However, a smaller Deutsch parameter accelerates relaxation, and we find a higher relaxation rate, especially for low values of r_s. The results of this study emphasizes the sensitivity of the relaxation rate relative to the choice of electron-ion potential used. This dependence of g on r_s can be understood in terms of the momentum-transfer cross section σ_t, which is proportional to the relaxation rate g [31]. The ratio of $\sigma_t(r_s)$, computed from the screened potential Eq. (1), over $\sigma_t(r_s=0)$, computed from the bare Coulomb potential, decreases monotonically from unity at $r_s=0$ as a function of r_s [32] in a similar fashion to the relaxation rate in Fig. 5. Therefore extrapolation of g to $r_s=0$ is the relaxation rate for the Coulomb potential from a purely classical MD simulation (a result independent of $\hbar$.) The Landau-Spitzer expression, Eq. (5), is derived from $\sigma_t(r_s=0)$. Using the ratio of $g(r_s)/g(r_s=\lambda_{ei})$ obtained from Fig. 5, an effective value of r_s can be deduced that reproduces the quantal relaxation rate from [12]. For point A in Table I, $g(BPS)/g(MD, r_s=\lambda_{ei}) = 1.49$. This ratio corresponds to the value of g at $r_s = 0.28\lambda_{ei}$ in Fig. 5. Interestingly, this semiclassical value for r_s is approximately equal to the value for $b_{\min} = 0.18\lambda_{ei}$ as derived from the analytical expression for g [12]. However, the situation is complicated by the distinction which should be made between screening of the nucleus from the electrons as implemented through the choice of r_s, and by plasma screening of the ions by the electronic charge cloud. The latter is automatically included in the MD simulations, but is not, in general, included in the MFGR calculations.

IV. CONCLUDING REMARKS

Using classical molecular dynamics, we have calculated the relaxation rate g for several points along a degeneracy line equivalent to the plasma conditions expected to be found at NIF (National Ignition Facility). We find that the MD simulations are in reasonable agreement with the rates from the Landau-Spitzer approach for $b_{\min} = \lambda_{ei}$ and are around 30% higher than calculations made using quantal Fermi golden rule approaches. We find that the relaxation rates are sensitive to the screening parameter used in the MD simulations. By inverting the classical MD relaxation rate, that employed the screened potential, against the quantal BPS [12] rate, a semiclassical value for the screening length $r_s = 0.28\lambda_{ei}$ is suggested.

Finally, we note that the relaxation rates for fully ionized dense hydrogen plasmas computed from the Fermi golden rule approach, and from the analytic expression of Brown *et al.* [12], are around 40% higher than the Landau-Spitzer formula (using $b_{\min}=\lambda_{ei}$) which is commonly used in fusion modeling. It would be of interest to study how these different relaxation rates impact on the modeling of the yield from inertial confinement fusion devices such as NIF. For partially ionized plasmas, or plasmas containing mixtures of ions, the relaxation rates are much more difficult to compute. Work on these problems is underway.

ACKNOWLEDGMENTS

Los Alamos National Laboratory is operated by Los Alamos National Security, LLC, for the National Nuclear Security Administration of the U.S. Department of Energy under Contract No. DE-AC52-06NA25396. We acknowledge support from the Advanced Simulation and Computing Program's Mix & Burn Theory Project at Los Alamos National Laboratory. We acknowledge fruitful discussions with D. Kilcrease, G. Dimonte, B. Singleton, L. Brown, J. Daligault, and D. Vrinceanu.

[1] L. D. Landau, Phys. Z. Sowjetunion **10**, 154 (1936).
[2] L. Spitzer, Mon. Not. R. Astron. Soc. **100**, 396 (1940).
[3] L. Spitzer, *Physics of Fully Ionized Gases* (Interscience, New York, 1967).
[4] H. Brysk, Plasma Phys. **16**, 927 (1974).
[5] Y. T. Lee and R. M. More, Phys. Fluids **27**, 1273 (1984).
[6] M. W. C. Dharma-wardana and F. Perrot, Phys. Rev. E **58**, 3705 (1998); **63**, 069901(E) (2001).
[7] M. W. C. Dharma-wardana, Phys. Rev. E **64**, 035401(R) (2001).
[8] Sh. Kogan, Fiz. Tverd. Tela (Leningrad) **4**, 2474 (1963); [Sov. Phys. Solid State **4**, 1813 (1963)].
[9] G. Hazak, Z. Zinamon, Y. Rosenfeld, and M. W. C. Dharma-wardana, Phys. Rev. E **64**, 066411 (2001).
[10] D. O. Gericke, M. S. Murillo, and M. Schlanges, Phys. Rev. E **65**, 036418 (2002).
[11] D. O. Gericke, J. Phys.: Conf. Ser. **11**, 111 (2005).
[12] L. S. Brown, D. L. Preston, and R. L. Singleton, Jr., Phys. Rep. **410**, 237 (2005).
[13] L. S. Brown and R. L. Singleton, Jr., Phys. Rev. E **76**, 066404 (2007).
[14] J. Daligault and D. Mozyrsky, Phys. Rev. E **75**, 026402 (2007).
[15] P. Celliers, A. Ng, G. Xu, and A. Forsman, Phys. Rev. Lett. **68**, 2305 (1992).
[16] A. Ng, P. Celliers, G. Xu, and A. Forsman, Phys. Rev. E **52**, 4299 (1995).
[17] D. Riley, N. C. Woolsey, D. McSherry, I. Weaver, A. Djaoui, and E. Nardi, Phys. Rev. Lett. **84**, 1704 (2000).
[18] J. M. Taccetti, R. P. Shurter, J. P. Roberts, J. F. Benage, B. Graden, B. Haberle, M. S. Murillo, B. Vigil, and F. J. Wysocki, J. Phys. A **39**, 4347 (2006).
[19] U. Reimann and C. Toepffer, Laser Part. Beams **8**, 771 (1990).
[20] J. P. Hansen, and I. R. McDonald, Phys. Lett. **97A**, 42 (1983).
[21] I. V. Morozov and G. E. Norman, J. Phys. A **36**, 6005 (2003).
[22] C. Kittel, *Introduction to Solid State Physics* (Wiley, New York, 1996).
[23] S. Ichimaru, *Statistical Plasma Physics I* (Addison-Wesley, Reading, MA, 1991), Vol. I.
[24] C. Deutsch, Phys. Lett. **60A**, 317 (1977); V. G. Kelbg, Ann. Phys. **12**, 219 (1963); **13**, 354 (1964); **14**, 394 (1964).
[25] B. Jeon, Ph.D. thesis, University of California, Davis, 2008.
[26] G. Csanak and W. Daughton, J. Quant. Spectrosc. Radiat. Transf. **83**, 83 (2004).
[27] C. Gouedard and C. Deutsch, J. Math. Phys. **19**, 32 (1978).
[28] J. L. Bretonnet and M. Boulahbak, Phys. Rev. B **53**, 6859 (1996).
[29] A. L. Fetter and J. D. Walecka, *Quantum Theory of Many-Particle Systems* (McGraw-Hill, New York, 1971), pp. 303–307.
[30] G. Csanak, M. Murillo, and W. Daughton, Los Alamos Report No. LA-UR-04-0346, 2004.
[31] D. Vrinceanu, J. D. Kress, and L. A. Collins (unpublished).
[32] L. D. Landau and E. M. Lifshitz, *Physical Kinetics* (Pergamon, Oxford, 1981).